Supplement of Atmos. Chem. Phys., 21, 12173–12187, 2021
https://doi.org/10.5194/acp-21-12173-2021-supplement

Atmospheric Chemistry and Physics
Open Access
EGU

Supplement of

Rapid mass growth and enhanced light extinction of atmospheric aerosols during the heating season haze episodes in Beijing revealed by aerosol–chemistry–radiation–boundary layer interaction

Zhuohui Lin et al.

Correspondence to: Yonghong Wang (yonghongwang@rcees.ac.cn)

1. CO_2^+/ NO_3 artefact correction of ACSM

Recently, it was discovered that NO_3 induces a positive bias on organic CO_2^+ concentrations in the AMS/ACSM systems, which can be described as a function of ambient NO_3 ($\mu g/m^3$) in combination with the CO_2^+/NO_3 ratio from pure NH_4NO_3 measurements $(CO_2^+/NO_3)_{AN}$:

For pure NH_4NO_3 aerosol from calibrations, we determined the magnitude of the CO_2^+/NO_3 artefact (Pieber et al., 2016) and parametrized it as a function of the fragmentation pattern of $NO_3(NO^+/NO_2^+)$ to account for changes in the vaporizer in the ACSM:

$$(CO_2^+/NO_3)_{NH4NO3} = 0.025 \pm 0.002 \times (NO^+/NO_2^+)_{NH4NO3}$$

Then we determined the CO_2 concentration from OA using a two week moving average (NO^+/NO_2^+) from ambient observations:

$$(CO_2^+)_{OA,meas} = (CO_2^+)_{meas} - (CO_2^+/NO_3)_{NH4NO3} \times (NO_3)_{meas}$$

2. Significance test of the increment during haze

We use the function ranksum of MATLAB to perform Wilcoxon rank-sum test.

p = ranksum(x,y) returns the p-value of a two-sided Wilcoxon rank sum test. ranksum tests the null hypothesis that data in x and y are samples from continuous distributions with equal medians, against the alternative that they are not. The test assumes that the two samples are independent. x and y can have different lengths.

This test is equivalent to a Mann-Whitney U-test.

The result h = 1 indicates a rejection of the null hypothesis, and h = 0 indicates a failure

to reject the null hypothesis at the 5% significance level.

Example:

p = ranksum(x,y)

p = 0.0375

The p-value of 0.0375 indicates that ranksum rejects the null hypothesis of equal medians at the default 5% significance level.

Species	p	h
AWC [µg/m^3]	5.4286*10^(-76)	1
NH3 [ppb]	1.2178*10^(-55)	1
HOMs [molecule/cm^3]	8.7649*10^(-42)	1
HONO [ppb]	2.1083*10^(-29)	1
EC [µg/m^3]	2.2462*10^(-61)	1
OC [µg/m^3]	2.83*10^(-82)	1
OH	6.1802^(-4)	1
NO3 [µg/m^3]	1.6328*10^(-91)	1
SO4 [µg/m^3]	6.5457*10^(-80)	1
NH4 [µg/m^3]	1.2669*10^(-91)	1
Cl [µg/m^3]	3.5606*10^(-63)	1
Org [µg/m^3]	1.2495*10^(-79)	1
$PM_{2.5}$ [µg/m^3]	8.0856*10^(-113)	1

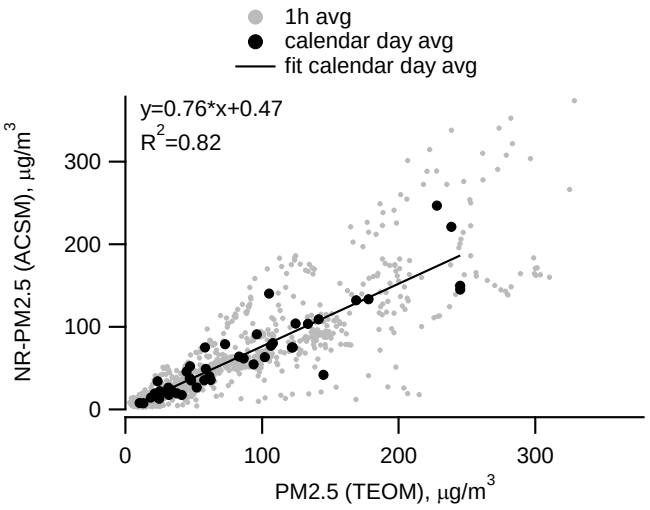

Figure S1. The relationship between $PM_{2.5}$ measured by TEOM and ToF-ACSM.

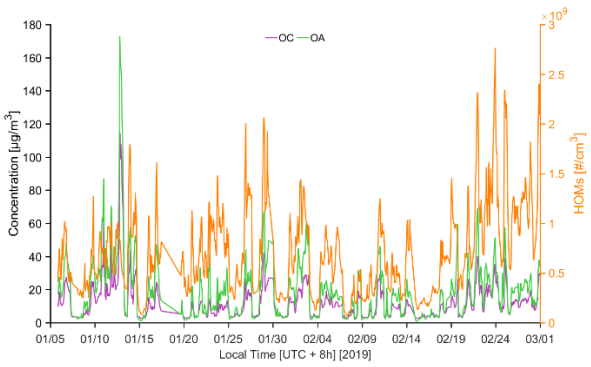

Figure S2. Time series of HOMs and OA measured by LTOFCIMS and ACSM, respectively.

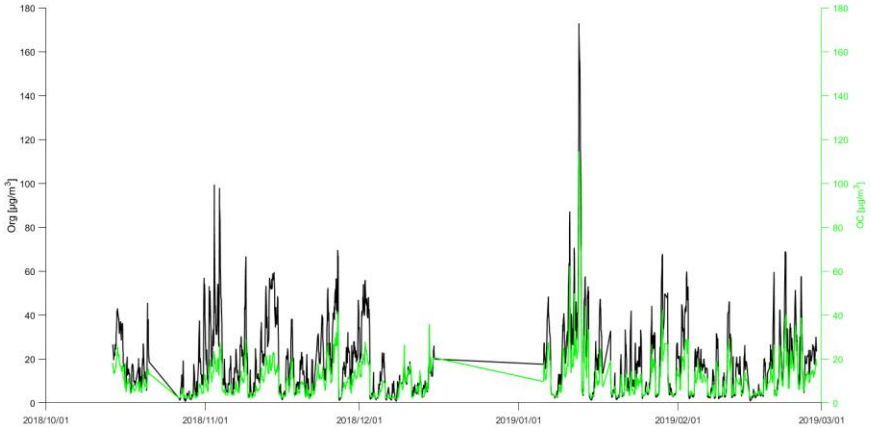

Figure S3. Time series of ToF-ACSM Org and Sunset OC.

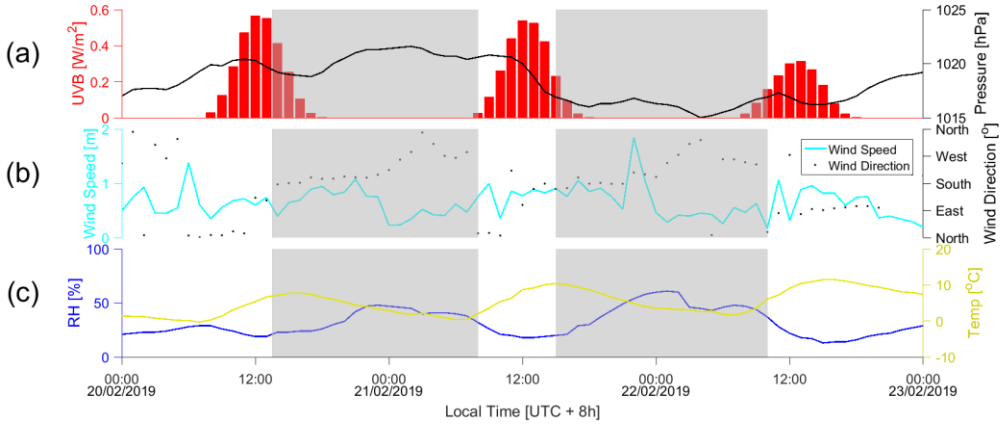

Figure S4. Time series of (a) ultraviolet radiation (UVB) and atmospheric pressure (P), (b) wind speed (WS) and wind direction (WD), and (c) relative humidity (RH) and temperature (T) during the observation period. The haze periods are marked by the shaded areas.

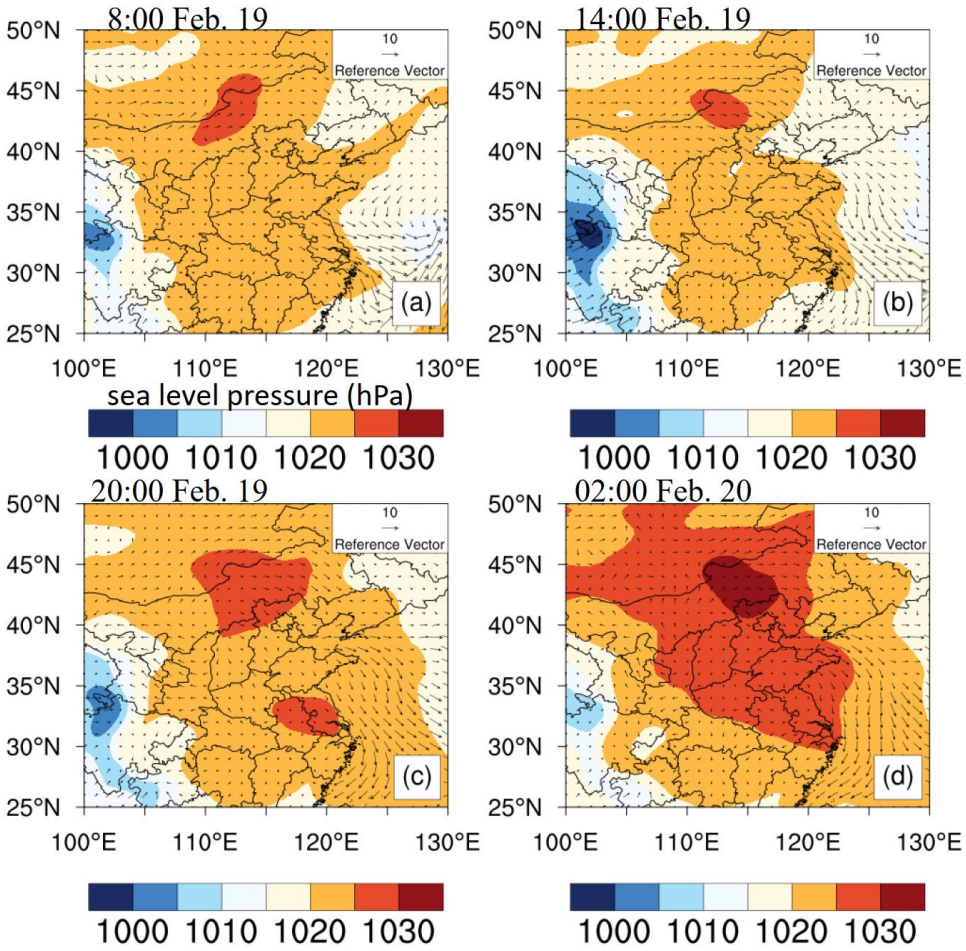
8:00 Feb. 19
14:00 Feb. 19
20:00 Feb. 19
02:00 Feb. 20
10
Reference Vector
(a)
(b)
(c)
(d)
50°N
45°N
40°N
35°N
30°N
25°N
100°E
110°E
120°E
130°E
sea level pressure (hPa)
1000 1010 1020 1030

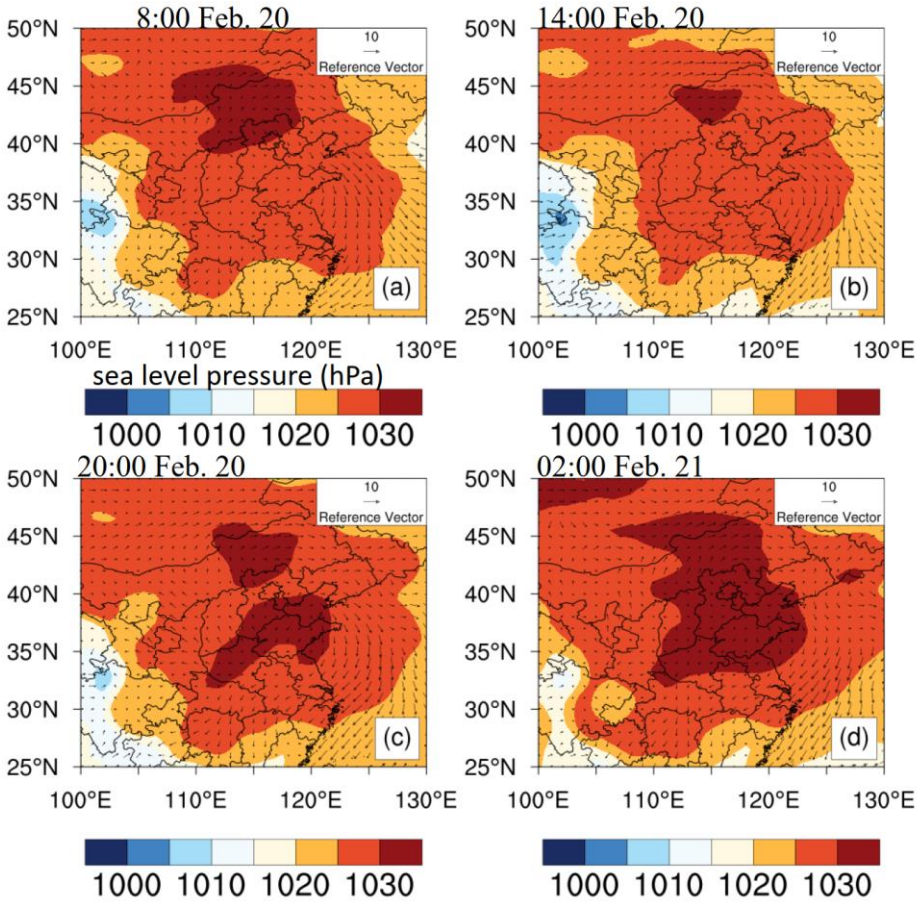
8:00 Feb. 20
14:00 Feb. 20
20:00 Feb. 20
02:00 Feb. 21
10
Reference Vector
(a)
(b)
(c)
(d)
50°N
45°N
40°N
35°N
30°N
25°N
100°E
110°E
120°E
130°E
sea level pressure (hPa)
1000 1010 1020 1030

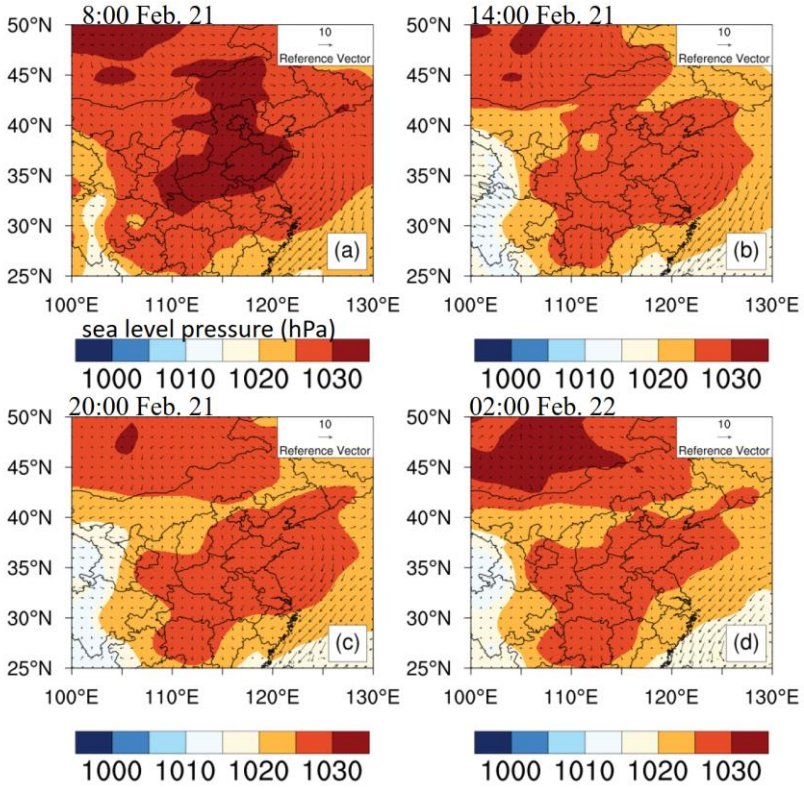
8:00 Feb. 21
14:00 Feb. 21
20:00 Feb. 21
02:00 Feb. 22
10
Reference Vector
(a)
(b)
(c)
(d)
50°N
45°N
40°N
35°N
30°N
25°N
100°E
110°E
120°E
130°E
sea level pressure (hPa)
1000 1010 1020 1030

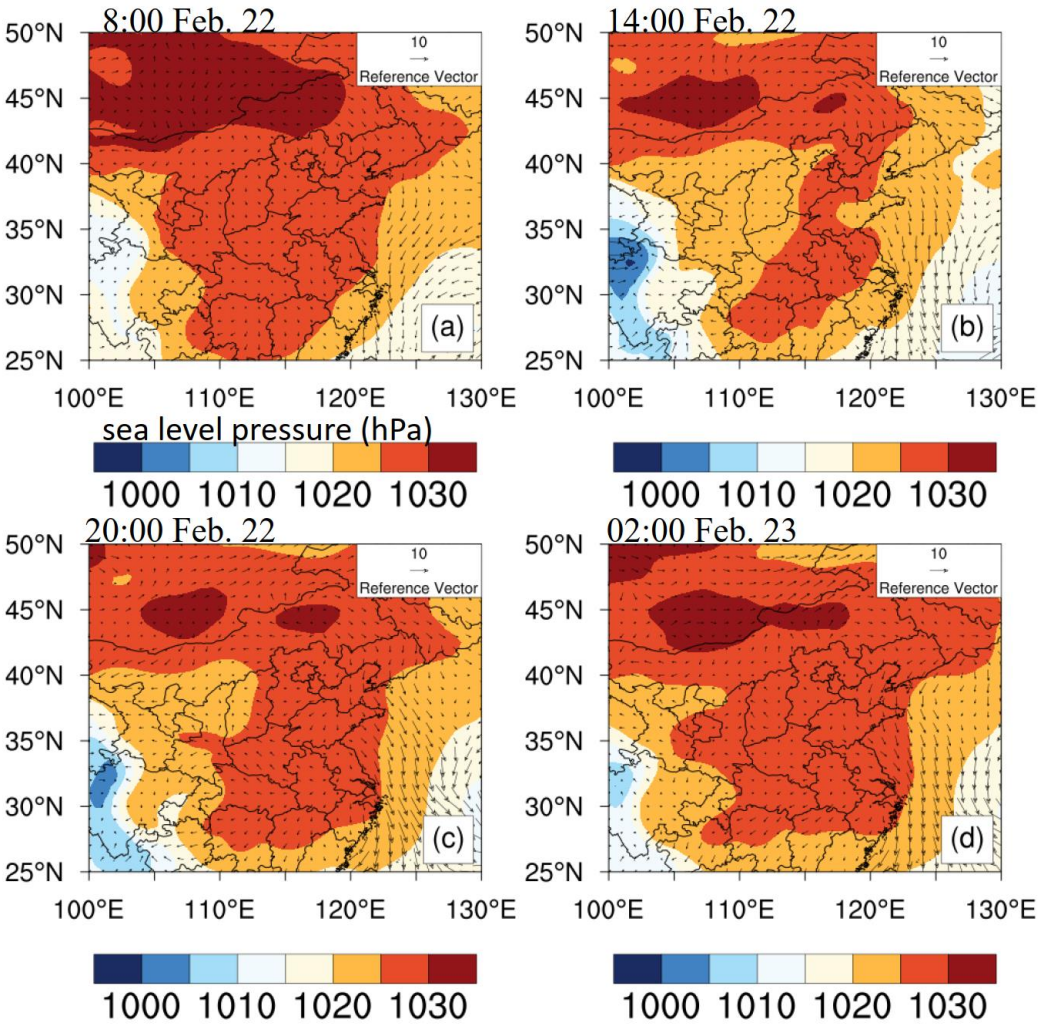

Figure S5. Composites of the sea level pressure field (units: HPa, shaded colors) and the ground wind field (units: m s^{-1}, black arrows) at different times, labeled as (a) - (d), during a typical haze period in BJ from February 19 to 22, 2019.

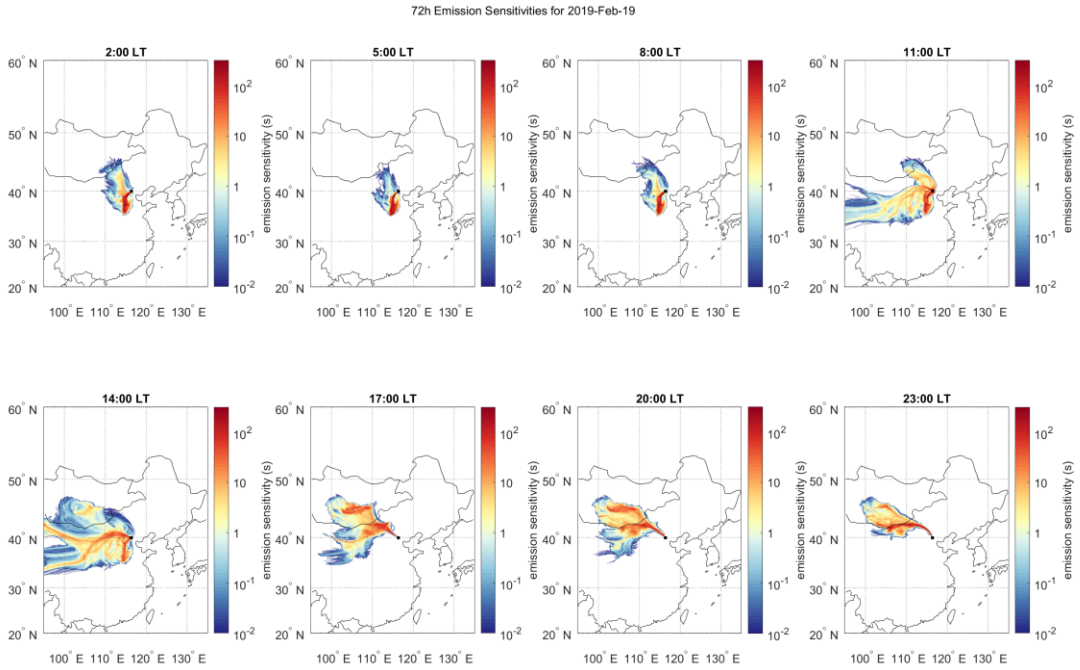
72h Emission Sensitivities for 2019-Feb-19
2:00 LT
5:00 LT
8:00 LT
11:00 LT
14:00 LT
17:00 LT
20:00 LT
23:00 LT
emission sensitivity (s)
60° N
50° N
40° N
30° N
20° N
100° E 110° E 120° E 130° E

(a)

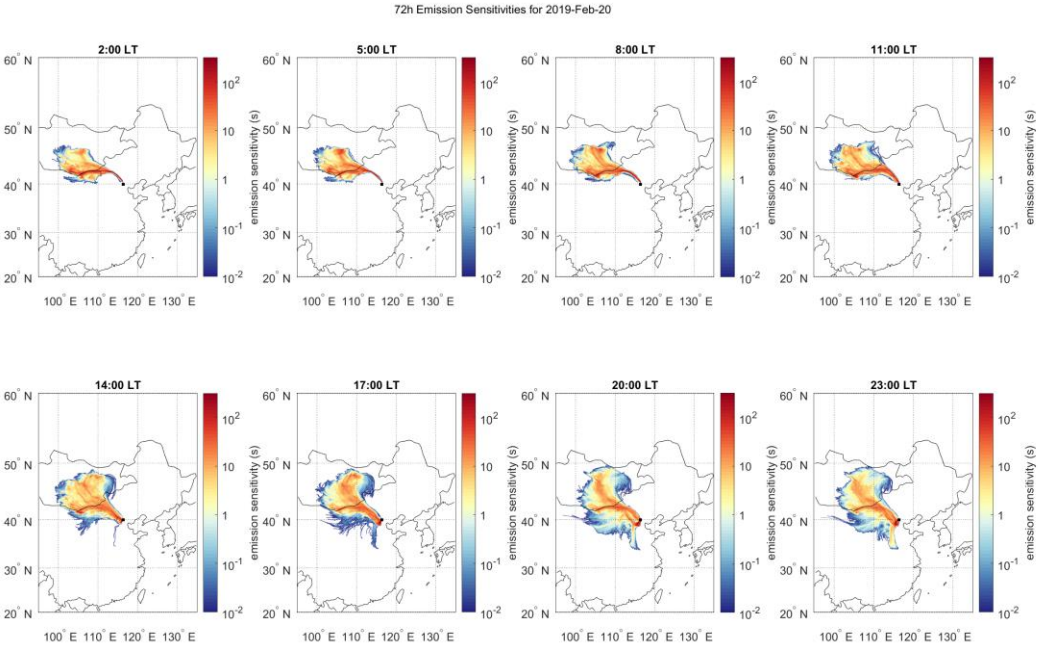
72h Emission Sensitivities for 2019-Feb-20
2:00 LT
5:00 LT
8:00 LT
11:00 LT
14:00 LT
17:00 LT
20:00 LT
23:00 LT
emission sensitivity (s)
60° N
50° N
40° N
30° N
20° N
100° E 110° E 120° E 130° E

(b)

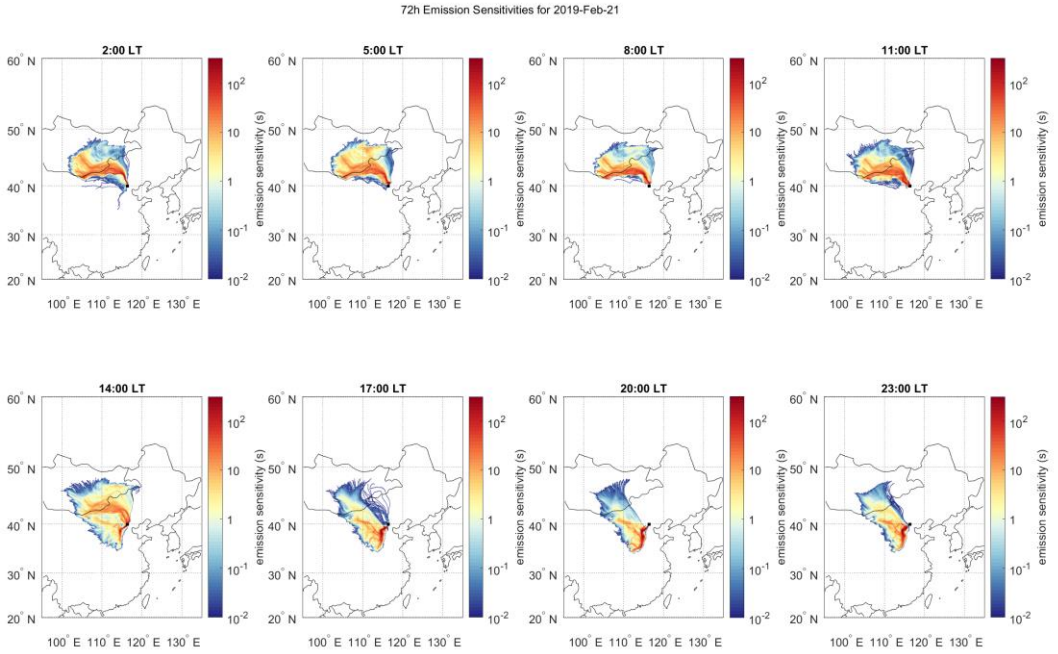

(c)

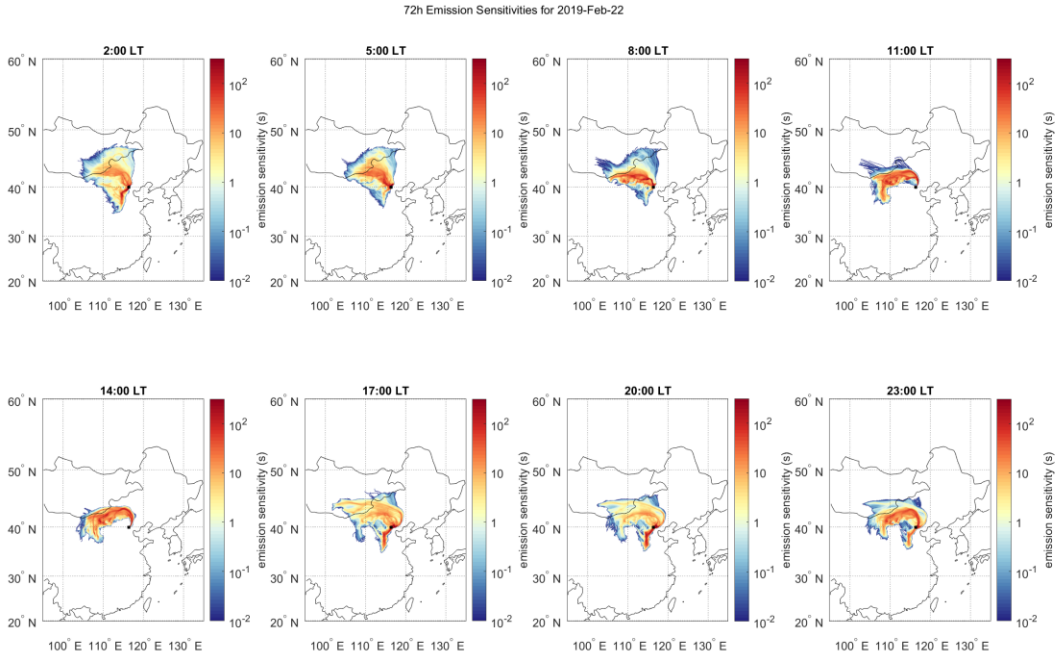

Figure S6. The 72 hour emission sensitivities (backward retro plumes) for the measurement period. The emission sensitivity values are proportional to the time that the air masses (model particles) have spent over a specific grid during their transport. The text above the figure panels indicates the particle release times in Beijing local time (LT). From these figures we can see that the polluted periods occur under southerly transport conditions, while the pollutants are cleared away during clean air masses from the north-easterly regions.

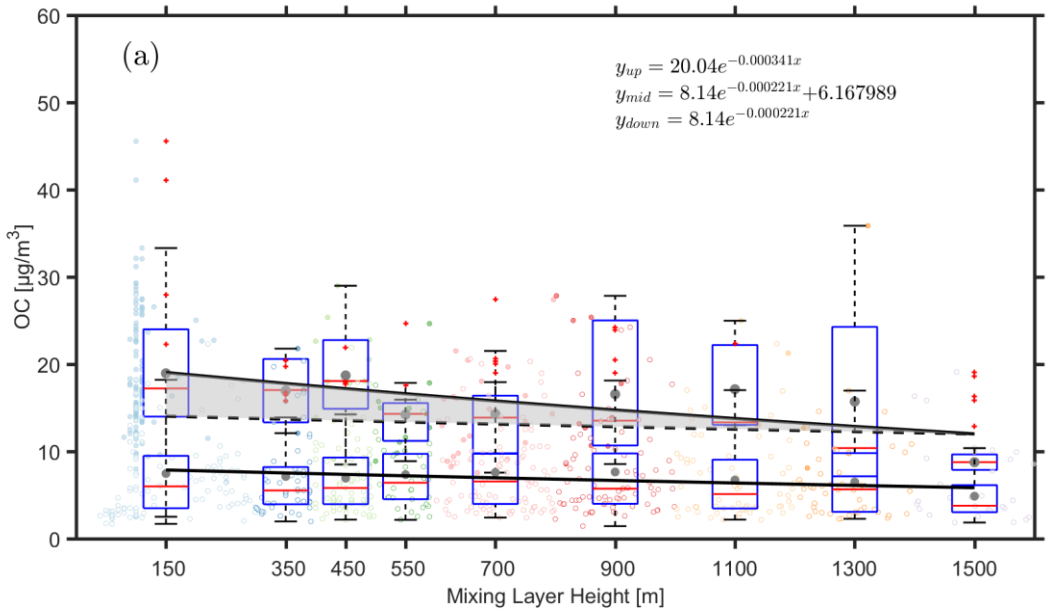
(a)
$y_{up} = 20.04e^{-0.000341x}$
$y_{mid} = 8.14e^{-0.000221x}+6.167989$
$y_{down} = 8.14e^{-0.000221x}$
OC [μg/m^3]
0
10
20
30
40
50
60
150
350
450
550
700
900
1100
1300
1500
Mixing Layer Height [m]

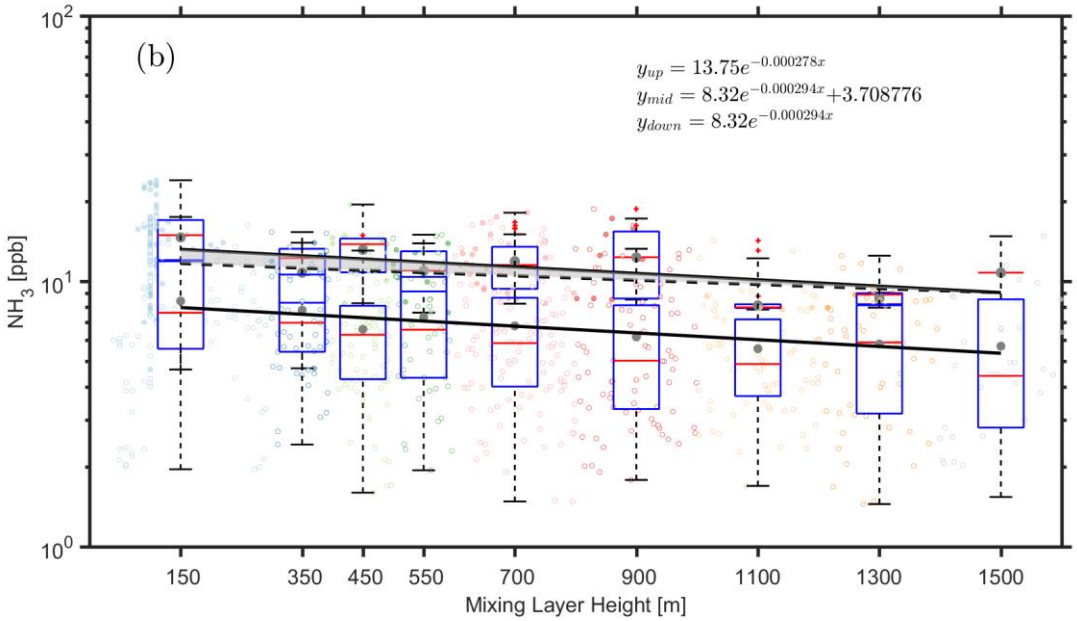
(b)
$y_{up} = 13.75e^{-0.000278x}$
$y_{mid} = 8.32e^{-0.000294x}+3.708776$
$y_{down} = 8.32e^{-0.000294x}$
NH$_3$ [ppb]
10^0
10^1
10^2
150
350
450
550
700
900
1100
1300
1500
Mixing Layer Height [m]

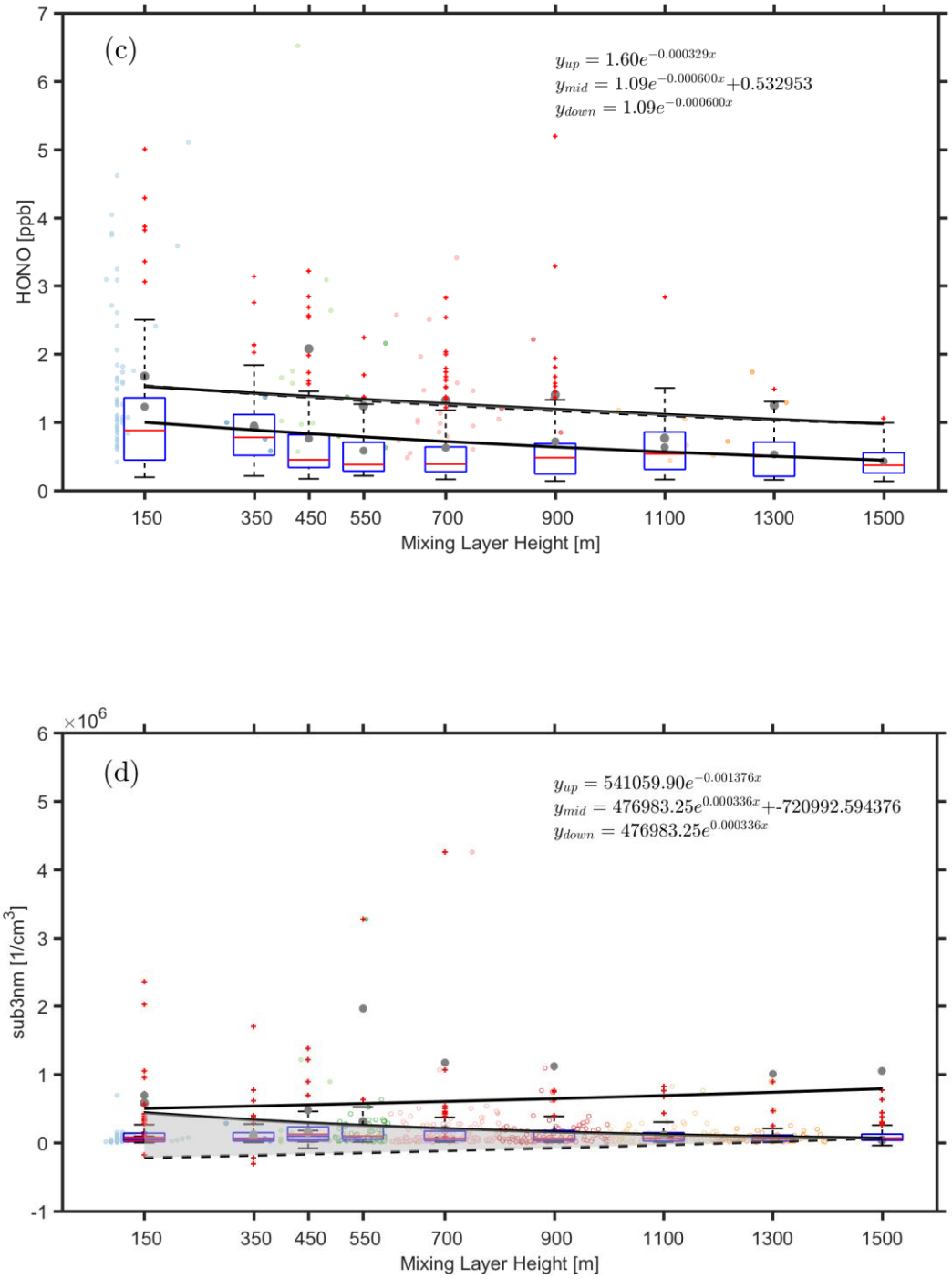

Figure S7. The dependence of different components (OC (a), NH_3 (b), HONO (c), nucleated cluster concentration of sub 3 nm (d)) during polluted and less-polluted conditions as a function of observed MLH. The data related to the upper fitting line represents $PM_{2.5}$ concentrations larger than 75 μg m^{-3}, while the date related to the lower fitting line represents $PM_{2.5}$ concentrations less than 75 μg m^{-3}. Only daytime conditions determined by the ceilometer from non-rainy periods (RH<95%) are considered. The dark grey points represent mean values; the red line represents median values. The shaded area corresponds to an increased amount of the specific compounds with decreased MLH assuming that the compound has the same variation pattern under highly- polluted conditions as in

less polluted time.

Table S1. statistics of the air pollutants used in the study.

Species	Mean	Min	Max	Standard deviation
HOMs [molecule/cm^3]	6.4557*10^8	6.5261*10^7	2.7647*10^9	4.3494*10^8
OC [μg/m^3]	11.0719	1.4217	114.3976	9.3642
NO3 [μg/m^3]	15.7131	0.0310	126.8300	22.1511
SO4 [μg/m^3]	5.5307	0.1951	117.5360	9.4079
NH4 [μg/m^3]	6.4492	0.0913	51.4603	8.5404
Cl [μg/m^3]	1.6346	0.0025	17.0581	1.9476
Org [μg/m^3]	19.1311	0.6662	172.8490	17.0184
$PM_{2.5}$ [μg/m^3]	50.8277	0.1592	218.5980	48.3780

Reference

[1] CAI J, CHU B, YAO L, et al. Size-segregated particle number and mass concentrations from different emission sources in urban Beijing [J]. Atmospheric Chemistry and Physics, 2020, 20(21): 12721-40.

[2] CRENN V, SCIARE J, CROTEAU P L, et al. ACTRIS ACSM intercomparison – Part 1: Reproducibility of concentration and fragment results from 13 individual Quadrupole Aerosol Chemical Speciation Monitors (Q-ACSM) and consistency with co-located instruments [J]. Atmospheric Measurement Techniques, 2015, 8(12): 5063-87.

[3] POULAIN L, SPINDLER G, GRüNER A, et al. Multi-year ACSM measurements at the central European research station Melpitz (Germany) – Part 1: Instrument robustness, quality assurance, and impact of upper size cutoff diameter [J]. Atmospheric Measurement Techniques, 2020, 13(9): 4973-94.

[4] FRENEY E, ZHANG Y, CROTEAU P, et al. The second ACTRIS inter-comparison (2016) for Aerosol Chemical Speciation Monitors (ACSM): Calibration protocols and instrument performance evaluations [J]. Aerosol Science and Technology, 2019, 53(7): 830-42.

[5] PETIT J E, FAVEZ O, SCIARE J, et al. Two years of near real-time chemical composition of submicron aerosols in the region of Paris using an Aerosol Chemical Speciation Monitor (ACSM) and a multi-wavelength Aethalometer [J]. Atmospheric Chemistry and Physics, 2015, 15(6): 2985-3005.

[6] PIEBER S M, EL HADDAD I, SLOWIK J G, et al. Inorganic Salt Interference on CO2(+) in Aerodyne AMS and ACSM Organic Aerosol Composition Studies [J]. Environ Sci Technol, 2016, 50(19): 10494-503.

[7] KEVIN ASHLEY P D A P F O C, NIOSH. NIOSH Manual of Analytical Methods (NMAM), 5th Edition

[M]. DEPARTMENT OF HEALTH AND HUMAN SERVICES Centers for Disease Control and Prevention National Institute for Occupational Safety and Health, 2016.
[8] BAUER J J, YU X Y, CARY R, et al. Characterization of the sunset semi-continuous carbon aerosol analyzer [J]. J Air Waste Manag Assoc, 2009, 59(7): 826-33.
[9] BROWN S G, LEE T, ROBERTS P T, et al. Variations in the OM/OC ratio of urban organic aerosol next to a major roadway [J]. J Air Waste Manag Assoc, 2013, 63(12): 1422-33.